ISSN: 1511-3701
Pertanika J. Trop. Agric. Sci. **34 (2)**: 351 - 361 (2011)

Histopathological Features of Peripheral T-cell Lymphoma in Sprague Dawley Rats Induced with *N*-methyl-*N*-nitrosourea

A.H. Hutheyfa[1], H. Hazilawati[1*], S.M. Rosly[2], S. Jasni[1], M.M. Noordin[1] and S. Shanmugavelu[2]

[1]Department of Veterinary Pathology and Microbiology,
Faculty of Veterinary Medicine, Universiti Putra Malaysia,
43400 UPM, Serdang, Selangor, Malaysia
[2]Strategic Livestock Research Centre,
Malaysian Agricultural Research and Development Institute,
43400 Serdang, Selangor, Malaysia
[*]E-mail: hazila@vet.upm.edu.my

ABSTRACT

This study described the histopathological features of peripheral T-cell lymphoma in male Sprague Dawley rats following intraperitoneal (i.p.) injections of *N*-methyl-*N*-nitrosourea (MNU) at a dose of 60 mg/kg body weight per injection, administered twice weekly for 2 consecutive weeks, and followed by a five-month's observation period. Control rats were injected with normal saline, i.p. All the rats treated with MNU had enlargement of lymph nodes, with 30% had hepatosplenomegaly and 7% had enlarged kidneys at necropsy. Malignant lymphoma was observed in the lymph nodes, spleen, liver, lung, heart, and kidneys. The neoplastic cells were characterised as undifferentiated, and small to large size with bizarre pleomorphic nuclei. The severity was further described as mild, moderate and severe, based on the diffuseness of the lesions. Nonetheless, similar lesions were not observed in the thymus of the rats. Immunohistochemistry staining of the organs was positive for CD3 antibody, which is consistent with T-cell lymphoma.

Keywords: *N*-methyl-*N*-Nitrosourea (MNU), rats, peripheral T-cell lymphoma

INTRODUCTION

Development of animal model for human lymphoma may provide a basis for investigating new biomarkers for early diagnosis and new anti-tumour therapies. Studies have shown that *N*-methyl-*N*-nitrosourea (MNU) induced lymphoma and leukaemia in rats (Koestner *et al*., 1977; Mizoguchi *et al*., 1993; da Silva Franchi *et al*., 2003; Hutheyfa *et al*., 2009a, b; Hazilawati *et al*., 2010a, b). The chemical is one of the *N*-nitroso compounds which is found in food and tobacco smoke (Fiddler, 1975; Beranek, 1990). It has a broad spectrum of the target organs including the lympho-haemopoietic system. Our preliminary study, for instance, has shown that this particular chemical induced stages IV and III lymphoma in young adult and adult male Sprague Dawley rats, respectively (Hutheyfa *et al*., 2009a).

Diagnosis of lymphoma is made based on microscopic examination of the lesions. It could be done either through cytological and/

Received: 2 September 2010
Accepted: 23 September 2010
[*]Corresponding Author

or histopathological examinations. Meanwhile, the final diagnosis of lymphoma could only be achieved through histological examination. The final diagnosis of disseminated lymphoma, which is mostly seen in cats (Hazilawati, unpublished), however, could be made through cytological evaluation of the fluid samples which were obtained from pleural cavity of the cats. In cases of generalised canine lymphosarcoma, confirmatory diagnosis could also be made cytologically, provided that an adequate number of malignant lymphocytes from the enlarged lymph nodes were aspirated (Hazilawati, unpublished). Cytological diagnosis of lymphoma in human and animals is always challenging, if adequate cells could not be obtained, which warrants a biopsy for histological evaluations. The objective of this study is to describe the pathological features of peripheral T-cell lymphoma in Sprague Dawley rats induced with MNU.

MATERIALS AND METHODS

Animals

Thirty-two 6-week-old male Sprague Dawley rats, with body weight ranging from 150 to 180 g, were obtained from the Laboratory Animal Resource Unit, Faculty of Medicine, Universiti Kebangsaan Malaysia (UKM) in Bangi, Selangor. The rats were placed in polypropylene plastic cages (two per cage) which were bedded with commercialised wood chips, and housed in a colony animal room with controlled conditions at the temperatures of 22-27°C, 40-70% humidity and 12-hours of light/dark lighting in the Animal House, at the Malaysian Agricultural Research and Development Institute (MARDI) in Serdang, Selangor. The rats were acclimatised for two weeks and fed with commercial rodent chows and drinking water ad *libitum* on a daily basis.

Chemical Carcinogen

N-methyl-*N*-nitrosourea (MNU) (Sigma-Aldrich®, N4766-25G) was used to initiate the carcinogenesis process. The chemical solution was freshly prepared by dissolving 14 mg of MNU in 1 mL of normal saline (pH 4.5).

Experimental Design

The rats were weighted and divided into two groups, with sixteen rats in each, after two weeks of acclimatisation. The MNU group received four intraperitoneal (i.p) injections, twice weekly for two consecutive weeks of MNU at a dose of 60 mg/kg of the body weight (the total dose received was 240 mg/kg of the body weight). Meanwhile, the control group was injected with normal saline, i.p. The rats were humanely sacrificed after 20 weeks of the experimental period by abdominal bleeding under anaesthesia with xylazine (100 mg/kg) and ketamine (40 mg/kg).

Organ Samples

Gross examination for the presence of tumor masses, and enlargement of lymph nodes and internal organs was performed at necropsy. Spleen, liver, lung, kidneys, thymus, and heart were immediately removed and blotted dry.

Histopathology

The necropsied samples were washed with cold normal saline and fixed in 10% formal buffered formalin for at least 48 hours. After fixation, the samples were trimmed at 5 mm thickness and placed in plastic cassettes before they were processed using a standard overnight method in an Automated Tissue Processor (Leica ASP300, Germany). The samples were embedded in paraffin using a Tissue Embedding Console System (Leica EG1160, Germany) via a routine method of paraffin embedding procedure. The tissue samples were sectioned at 4 um thicknesses using a microtome (Leica RM2155, Germany). The tissue sections were placed on water bath (Leica H1210, Germany) at 35°C to 37°C, mounted on glass slides using a hot plate (Leica HI1220, Germany) and stained with Haematoxylin and Eosin (H&E) stain, as described by Luna (1968).

Immunohistochemistry

In this study, the immunohistochemistry analysis was performed using a Dako Envision®+Dual Link System-HRP (DAB+) kit (Dako, USA, Cn: K4965), as per manufacturer's instruction. The kit contains a blocking agent, secondary antibody labelled to horseradish peroxidase and diaminobenzidine [DAB]). The primary antibody (rabbit polyclonal to CD3 primary antibody, ab5690, ABcam®, USA) directed against CD3 (T-lymphocyte marker), was used to classify the lineage of the neoplastic cells in the necropsied organs. The primary antibody was spun in a centrifuge machine (Hettich mikro-120, Germany) at 12000 rpm for 20 seconds before it was diluted at a 1:100 dilution with antibody diluent and background reducing components (Dako, S3022). The paraffinised embedded sample sections for CD3 staining was pre-treated by steaming at 97°C in the target retrieval buffer (Dako, S3001) for 25 minutes. The tissue sections were incubated with anti-CD3 antibody for 30 minutes at room temperature. CD3 immunoreactivity was detected using the labelled polymer-HRP reagent (horseradish peroxidase labeled polymer conjugated to goat anti-rabbit and goat-anti-mouse secondary antibody) and visualised with DAB. All the immunohistochemical sections were counterstained with Mayer's hematoxylin, dehydrated in graded concentrations of ethanol (70%, 90%, and 100%), and cover slipped routinely using permanent mounting medium. The tissue sections were then examined under 10, 20, and 40x magnifications using a light microscope.

RESULTS AND DISCUSSION

N-methyl-*N*-nitrosourea (MNU) is one of carcinogens that has been used for induction of lymphoma and leukaemia (Joshi & Frei, 1970; Koestner *et al*., 1977; Baines *et al*., 1979; Uwagawa *et al*., 1991; Hagiwara *et al*., 1993; Mizoguchi *et al*., 1993; da Silva Franchi *et al*., 2003; Marton *et al*., 2008; Hutheyfa *et al*., 2009a, b; Hazilawati *et al*., 2010a, b), thymomas (Frei,1980), mammary gland (Esendagli *et al*., 2009), prostate (McCormick *et al*., 1999) and gastrointestinal (Mizoguchi *et al*., 1993; Tuncel *et al*., 2002) cancers in laboratory animals.

The type of cancer developed is dependent on the age, sex and strain of the laboratory animals, route of administration, concentration and the total dose of MNU, as well as the duration of the experimental period. Rats induced with MNU at young age (4 to 6-week-old) were reported to develop higher incidence of thymic lymphoma (Swenberg *et al*., 1975; Koestner *et al*., 1977; Mizoguchi *et al*., 1993) compared to middle-aged (52-week-old) and old age (98-week-old) rats (Mizoguchi *et al*., 1993). In particular, the middle-aged rats were found to likely to develop higher (97 - 100%) incidence of adenocarcinomas in the small intestine compared to young and old age rats (Mizoguchi *et al*., 1993). However, the administration of high dose of MNU (70 mg/kg body weight per injection for four injections) in young rats was found to have induced sub-acute haemolytic anaemia rather than lymphoma or leukaemia (Hazilawati *et al*., 2009).

The results of this study showed that all the rats treated with MNU (2 died during the experimental period) had enlargement of the lymph nodes, with 30% of the rats had hepatosplenomegaly and 7% had enlarged kidneys at necropsy. The organs were infiltrated with malignant lymphocytes in different grades, which were consistent with stage IV lymphoma, as described in the WHO's classification of human lymphoma (Jaffe *et al*., 2001). Meanwhile, normal architecture of those organs was diminished. Ironically, similar lesion was not observed in the thymus of all rats that had been treated with MNU. Using similar chemical, thymic lymphoma was observed in other studies (Koestner *et al*., 1977; Uwagawa *et al*., 1991; Hagiwara *et al*., 1993; Mizoguchi *et al*., 1993; da Silva Franchi *et al*., 2003).

It is important to note that the immunohistochemistry staining of the organs was positive for CD3 (*Fig. 1*), which is consistent with T-cell lymphoma. The results were comparable to those reported by Grompe *et al*. (1985), Kerja & Seidel (1986) and Marton *et al*.

(2008). However, they stated that most of the mice treated with MNU i.p developed thymic T-cell lymphoma as compared to peripheral T-cell lymphoma in this study.

The histopathological features of the T-cell lymphoma of spleen, lymph nodes, liver, lung, heart, and kidneys in this study were described as mild, moderate, and severe. In spleen, the malignant lymphocytes were generally characterised as undifferentiated, medium sized, bizarre pleomorphic nuclei with numerous mitotic figures in the red and white pulps (*Fig. 2*). The lesions were scored as mild as the malignant lymphocytes were individually present in the red pulp sinusoids and/or present as small focal aggregates in the splenic parenchyma. Normal architecture of the spleen was still preserved. Moderate lymphoma lesions were scored as the malignant lymphocytes surrounded the splenic cords in the red pulp and/or present as large focal aggregates in the spleen as well as in the periarterial lymphatic sheaths (PALS) which led to the enlargement of the white pulp. Other than those criteria, the presence of giant tumour cells and haemosiderin-laden macrophages in the red pulp are also important criteria. Severe lymphoma lesions were characterised by massive proliferation of malignant lymphocytes in the red and white pulps, leading to the loss of normal splenic architecture denoted by the absence of sinusoids and splenic cord in the red pulp, as well as marginal and follicular zones in the white pulp.

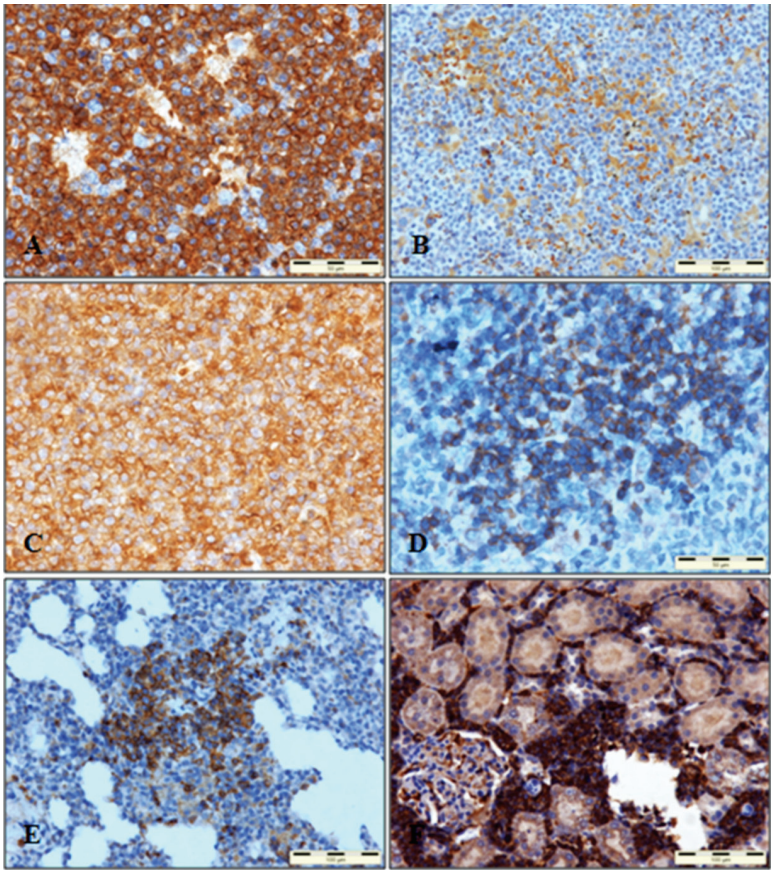

Fig. 1: Malignant T-lymphocytes in the lymph node (A), liver (B), spleen (C&D), lung (E) and kidney (F) stained positively for CD3 primary antibody

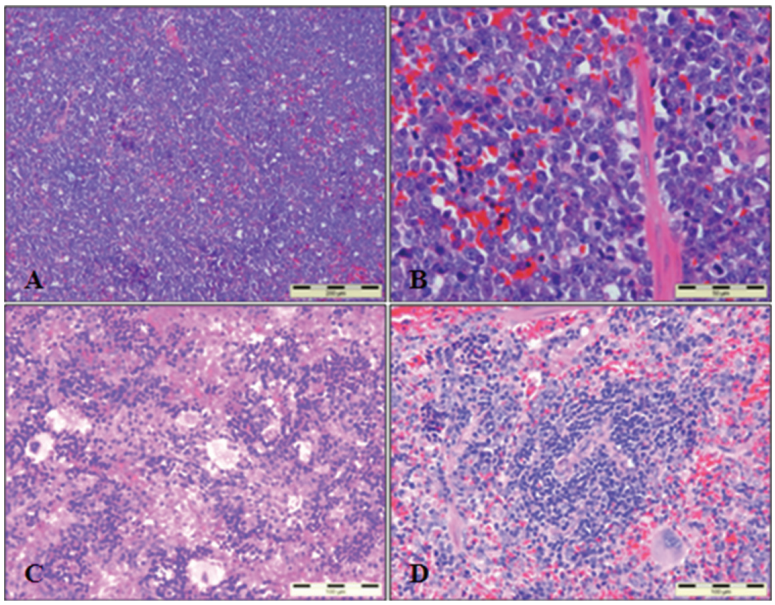

Fig. 2: Spleen; A&B) Normal architecture of the spleen, replaced by proliferation of numerous malignant lymphocytes (x10 & x40, respectively, H&E). C&D) Clusters of malignant lymphocytes in the red pulb (x20, H&E). Note one giant tumour cell in photomicrograph D and neoplastic lymphocytes surrounding the splenic cords in photomicrograph A to D

Generally, malignant lymphocytes in the lymph nodes, including auxiliary, mesenteric and submandibular, showed a similar criterion of malignancy as described in the spleen (*Fig. 3*). Meanwhile, mild lymphoma lesions were characterised as the presence of small focal aggregates of malignant lymphocytes in the paracortex and medullary areas of the lymph nodes. Infiltration of the malignant lymphocytes was occasionally observed in the subcapsular sinus. Moderate lymphoma lesions were described as the presence of large aggregates of malignant lymphocytes in the cortex, paracortex and medullary areas of the lymph nodes, leading to a partial loss of the normal lymph node architecture. Moderate infiltration of the malignant lymphocytes was observed in the subcapsular sinus. Severe lesions were denoted as the architecture of the cortex, paracortex, and medullary areas of the lymph nodes are diminished as a result of diffuse proliferation of malignant lymphocytes. The newly developed small blood vessels indicating angiogenesis were clearly observed in the lymph nodes. The subcapsular sinus was numerously proliferated by malignant lymphocytes and formed a neoplastic zone surrounding the lymph nodes.

Just like the spleen and lymph nodes, liver was infiltrated with malignant lymphocytes with a prominent criterion of malignancy. The size of the malignant lymphocytes varies from small to large. Hepatocytes were necrotised and congested (*Fig. 4*). Mild lesions were characterised as the presence of only a few malignant lymphocytes at the portal triads, necrotic hepatocytes with pyknotic nuclei and congested blood vessels. Moderate lesions were described as the presence of aggregates of malignant lymphocytes at the portal triads and also in the hepatic sinusoids, necrotic hepatocytes with karyorrhexis and karyolytic nuclei, and congestion of the blood vessels and hepatic sinusoids. Severe lesions were characterised as the presence of diffuse infiltration of malignant lymphocytes in the liver parenchyma. Hepatocytes were absent and/or only present as a small island, with 1 to

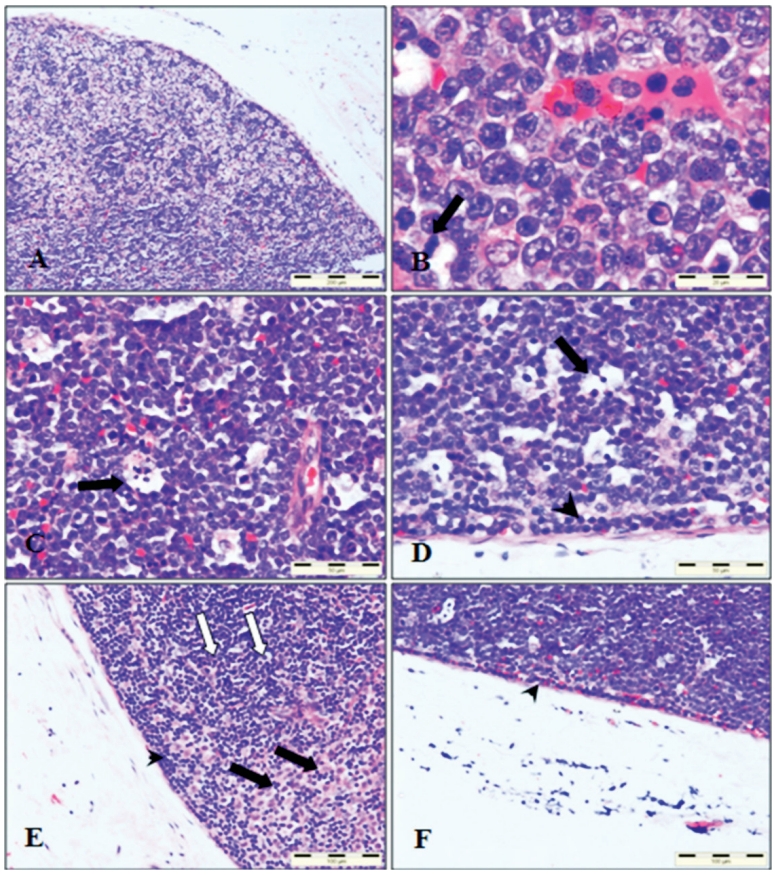

Fig. 3: Lymph node; A) Normal lymph node architecture is replaced by diffuse proliferation of small and large lymphocytes produces inconspicuous demarcation of structures in the cortex, which include trabeculae, lymphoid follicles and germinal centre, and medulla (x10, H&E). B) Numerous malignant lymphocytes characterised as marked cellular and nuclear pleomorphism (x100, H&E). Note that one mitotic figure (arrow). C & D) Numerous small blood vessels indicating angiogenesis (arrows) and infiltration of numerous malignant lymphocytes in the subcapsular sinus (arrow head) (x40, H&E). E & F) The subcapsular sinus (arrow heads) is infiltrated by malignant lymphocytes. E) Mixture of small (white arrows) and large lymphocytes (black arrows); nuclei of the large lymphocytes are paler and bigger indicating the cells are undergoing active proliferation (x20, H&E) (photomicrograph B, C, D, E, and F are magnification of photomicrograph A)

3 hepatocytes within the clusters of malignant lymphocytes. Meanwhile, liver parenchyma was severely congested.

Kidneys exhibited similar malignant lymphocyte characteristics as the spleen, lymph nodes and liver. The size of the malignant lymphocytes, however, varies from small to medium. The cells predominantly infiltrated into the interstitial space of the renal tubules, moderately infiltrated and surrounded the glomeruli. Numerous malignant lymphocytes were observed around the renal artery. Tubular epithelial necrosis was also observed (*Fig. 5*). Mild lymphoma lesions were characterised by the presence of metastatic neoplastic lymphocyte infiltration surrounding the large blood

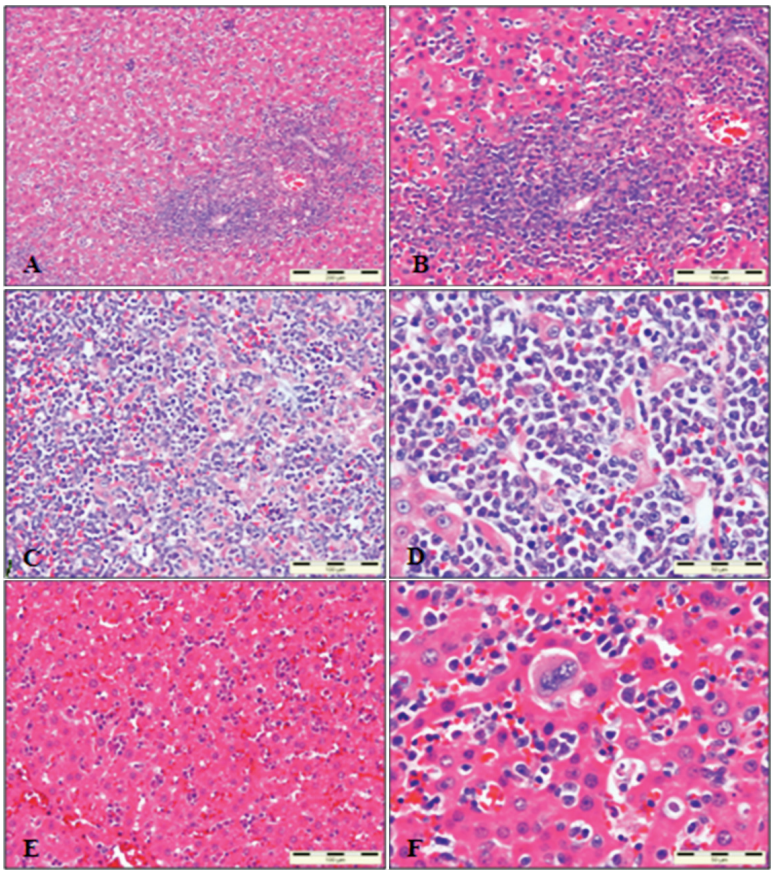

Fig. 4: Liver; A&B) Infiltration of numerous malignant lymphocytes at the portal triad area and in the hepatic sinusoids (x10 & x20, respectively, H&E). Note the congested blood vessel with malignant lymphocytes. C&D) Normal architecture of hepatocytes is replaced by diffuse infiltration of malignant lymphocytes (x20 & x40, respectively, H&E). Note that congested sinusoids and islands of hepatocyte surrounded by the malignant lymphocytes. E&F) Clusters of malignant lymphocytes in the hepatic sinusoids (x20 & x40, respectively, H&E). Note that one giant tumour cell in photomicrograph E (photomicrograph B, D and F are magnification of photomicrograph A, C and E, respectively)

vessels. For moderate lesions, similar lesions characterised for the mild lesions were observed, along with the presence of metastatic neoplastic lymphocyte infiltration in the renal interstitium of both cortex and medulla, as well as around the glomeruli. Congested blood present in the renal interstitium and large blood vessels. Epithelial necrosis of the renal tubules, which include the proximal, distal and loop of Henle, was occasionally observed. Severe lesions were described as the presence of predominantly medium sized metastatic neoplastic lymphocytes in the areas described for the mild and medium lesions, including the fatty tissue of the renal calyx/pelvis. The number of cells, however, was more abundant, which resulted in the reduction of the number of renal tubules. Congested blood in the large blood vessels contained numerous metastatic lymphocytes.

Lymphoma lesions in the lungs were exhibited by the infiltration of undifferentiated, small to medium size metastatic neoplastic

lymphocytes, with pleomorphic nuclei and mitotic activity, around the pulmonary blood vessels and as focal aggregates in the lung parenchyma. The clusters of neoplastic lymphocytes were also observed in the bronchus associated lymphoid tissue (BALT), leading to the enlargement of BALT (*Fig. 6*). Mild lymphoma lesions were characterised as the presence of a few number of small metastatic neoplastic lymphocytes around the large blood vessels. Moderate lymphoma lesions were observed by the presence of small to medium metastatic neoplastic lymphocytes around the pulmonary blood vessels and as small focal aggregates in the alveolar areas, resulting in the thickening of the alveolar walls. Meanwhile, enlargement of the BALT was observed as a result of the proliferation of the neoplastic lymphocytes. The cells were also observed to be present in the congested blood vessels and in the alveolar walls. For severe lesions, lung parenchyma was predominantly infiltrated by the neoplastic cells as large focal aggregates throughout the lung parenchyma, surrounding

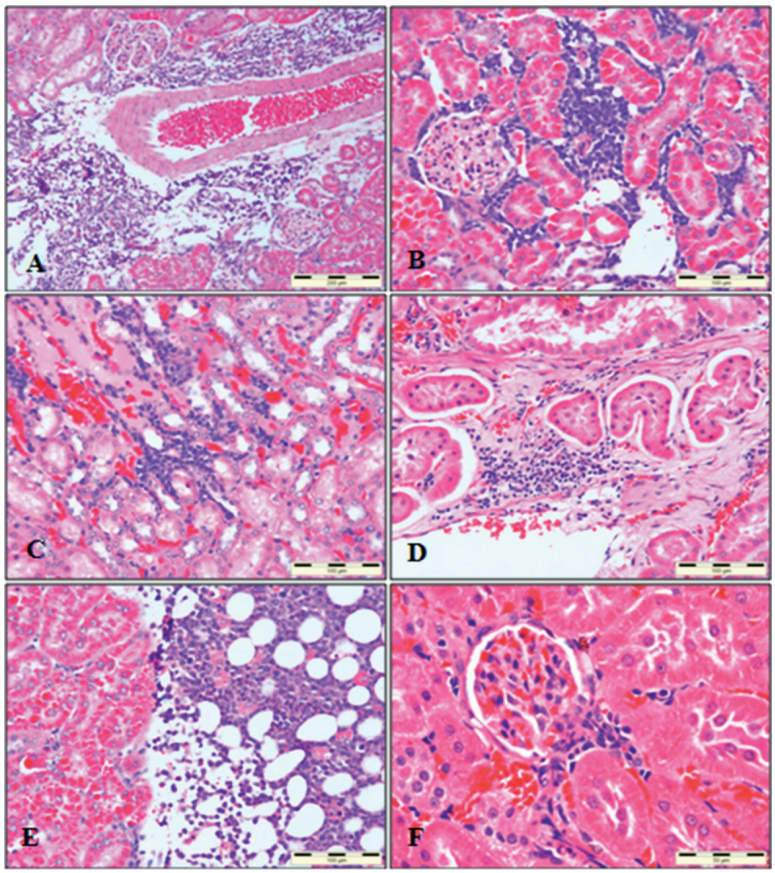

Fig. 5: Kidney; A) Infiltration of numerous malignant lymphocytes around the large blood vessel (x10, H&E). Note that the congested blood in the lumen of the renal artery contains malignant lymphocytes. (B, C & D) The malignant lymphocytes predominantly infiltrated the interstitial tissues of the renal tubules (x20, H&E). Note that the congested blood within the renal interstitial tissues in photomicrograph C. E) Infiltration of numerous malignant lymphocytes into the fatty tissues of the renal calyx/pelvis (x20, H&E). (B&F) Infiltration of the malignant lymphocytes surrounding/in the glomerulus (x40, H&E)

the small and large pulmonary blood vessels and also in the alveolar walls. The cells were proliferated in the BALT and this resulted in the enlargement of the BALT and the narrowing of the bronchial lumen. Congested blood with neoplastic lymphocytes and interstitial penuemonia were also noted.

The infiltration of metastatic neoplastic lymphocytes between the cardiac muscles was observed in the heart. Mild lesions were characterised as the presence of the neoplastic lymphocytes surrounding the coronary blood vessels. Moderate lesions were demonstrated as the presence of the neoplastic cells in between the cardiac muscles and also surrounding the blood vessels. Necrosis of the myocytes which led to loss of the normal myocyte coordination was also observed. Similar lesions were more obvious for severe lymphoma lesion in the heart, along with the aggregations of infiltrated neoplastic cells in the cardiac parenchyma (*Fig. 7*).

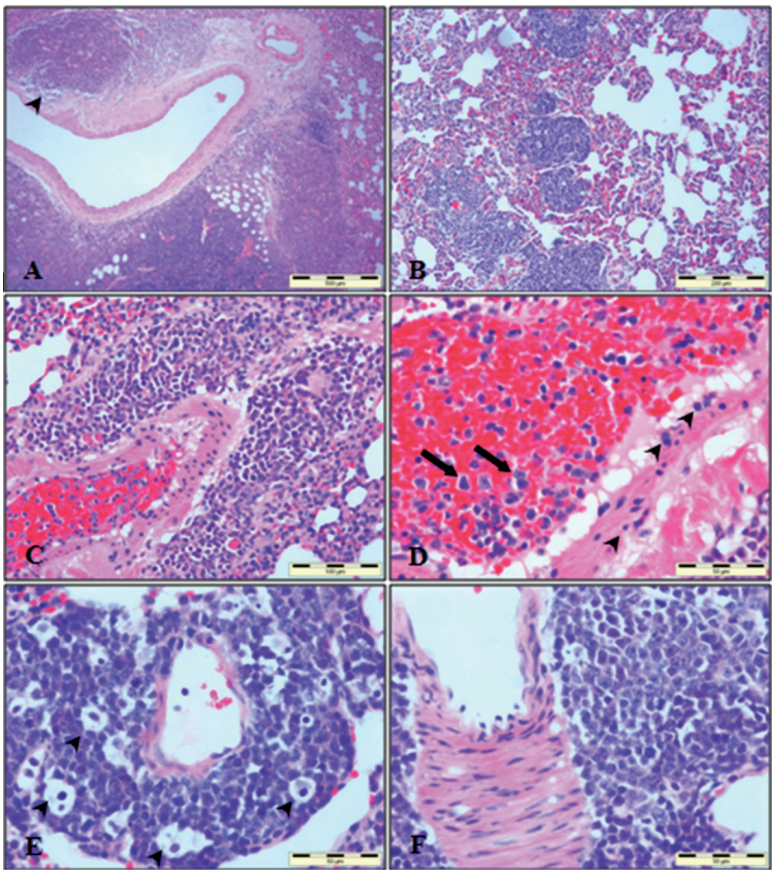

Fig. 6: Lung; A) Aggregation of malignant lymphocytes in BALT (arrowhead) (x4, H&E). B) Clusters of malignant lymphocytes infiltrated into the lung parenchyma (x10, H&E). C) Infiltration of numerous malignant lymphocytes around the pulmonary artery (x20, H&E). Note that presence of congested blood and malignant lymphocytes in the lumen of the pulmonary artery. D) Higher magnification of photomicrograph C clearly shows that the malignant lymphocytes are in the lumen (arrows) and wall (arrowheads) of the pulmonary artery (x40, H&E). E&F) The malignant lymphocytes are around the large and small blood vessels (arrowheads) (x40, H&E)

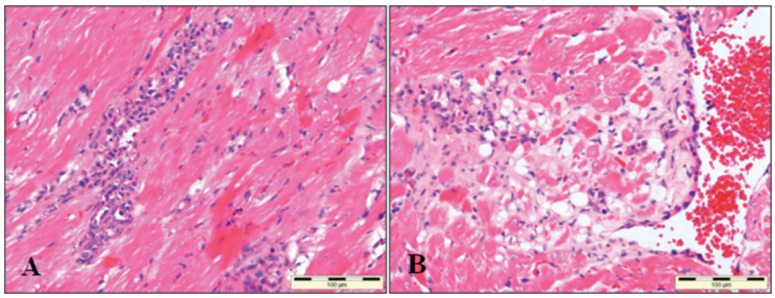

Fig. 7: Heart; A) Infiltration of malignant lymphocytes in between the cardiac muscles (x20, H&E). B) Fatty necrosis of the myocytes was observed around the large blood vessel which is infiltrated by the malignant lymphocytes (x20, H&E). Note that metastatic malignant lymphocytes line the intima of the large blood vessel. The congested large blood vessel contains a few malignant lymphocytes

CONCLUSION

The pathological features of stage IV peripheral T-cell lymphoma in rats, induced with MNU in different grades, have exclusively been described in this study. It is very useful for future study, particularly to evaluate the effectiveness or efficacy of new anti-tumor therapies.

ACKNOWLEDGEMENTS

The authors wish to express their gratitude to the Ministry of Higher Education (MOHE), Malaysia, for the FRGS grant (03-10-07-335FR), and the technical staff at the Animal House, Malaysian Agricultural Research and Development Institute (MARDI), Serdang, the Veterinary Haematology and Clinical Biochemistry Laboratory, and the Veterinary Histopathology Laboratory, Universiti Putra Malaysia (UPM), Serdang, Malaysia, for their excellent technical assistance.

REFERENCES

Baines, P., Dexter, T.M., & Schofield, R. (1979) Characterization of malignant cell population in MNU-induced leukemia in mice. *Leukemia Research*, *3*, 23-28.

Beranek, D.T. (1990). Distribution of methyl and ethyl adducts following alkylation with monofunctional alkylating agents. *Mutation Research*, *231*, 11-30.

da Silva Franchi, C.A., Bacchi, M.M., Padovani, C.R., & de Camargo, J.L. (2003). Thymic lymphomas in Wistar rats exposed to *N*-methyl-*N*-nitrosourea (MNU). *Cancer Science*, *94*, 240-243.

Fiddler, W. (1975). The occurrence and determination of n-nitrosocompounds. *Toxicology and Applied Pharmacology*, *31*, 352-360.

Esendagli, G., Yilmaz, G., Canpinar, H., Gunel-Ozcan, A., Guc, M.O., & Guc, D. (2009). Coexistence of different tissue tumourigenesis in an NMU-induced mammary carcinoma model: A histopathological report in Sprague-Dawley rats. *Laboratory Animals*, *43*, 60-64.

Frei, J.V. (1980). Methylnitrosourea induction of thymomas in AKR mice requires one or two hits only. *Carcinogenesis*, *1*, 721-723.

Grompe, M., Kerja, L., Schmidt, J., & Seidel, H.J. (1985). RNA virus expression during and after MNU-induced T cell leukemogenesis in mice. *Bulletin*, *51*, 377-384.

Hagiwara, A., Tanaka, H., Imaida, K., Tamano, S., Fukushima, S., & Ito, N. (1993). Correlation between medium-term multi-organ carcinogenesis bioassay data and long-term observation results in rats. *Japanese Journal of Cancer Research*, *84*, 237-245.

Hazilawati, H., Abdullah, M., Hutheyfa, A.H., Rosly, S.M., Jasni, S., Noordin, M.M., & Shanmugavelu, S. (2009). High concentration of *N*-methyl-*N*-nitrourea induced intravascular haemolytic anaemia rather than leukaemia/

lymphoma in Sprague Dawley rats. In *Proceedings of the 1st Malaysian Veterinary Association Pathology Conference* (pp. 95-99). Harbour View Hotel, Kuching Sarawak: Malaysian Association of Veterinary Pathologist.

Hazilawati, H., Hutheyfa, A.H., Rosly, S.M., Jasni, S., Noordin, M.M., & Shanmugavelu, S. (2010a). Haematological parameters of leukaemic rats supplemented with *Morinda citrifolia*. *The Malaysian Medical Journal*, *65*, 125-126.

Hazilawati, H., Nursyuhada, H., Hutheyfa, A.H., Rosly, S.M., Shanmugavelu, S., Noordin, M.M., & Jasni, S. (2010b). Effect of *Morinda citrifolia* on early stage of leukaemia in rats. *The Malaysian Medical Journal*, *65*, 135-136.

Hutheyfa, A.H., Hazilawati, H., Rosly, S.M., Jasni, S., Noordin, M.M., & Shanmugavelu, S. (2009a). *N*-methyl-*N*-nitrosourea induced stage III and IV lymphoma in male Sprague Dawley rats. In *Proceedings of the 21st Scientific Congress* (pp. 363-365). The Legend Water Chalets, Port Dickson, Negeri Sembilan: Veterinary Association Malaysia.

Hutheyfa, A.H., Hazilawati, H., Rosly, S.M., Jasni, S., Noordin, M M., & Shanmugavelu, S. (2009b). *N*-Methyl-*N*-Nitrosourea induced leukaemia in male Sprague-Dawley rats. In *Proceedings of the International Conference on Animal Health and Human Safety* (pp. 214-218). The Palm Garden Hotel IOI Resort, Putrajaya, Malaysia: Faculty of Veterinary Medicine Universiti Putra Malaysia-Airlangga University Indonesia-Department of Veterinary Services Malaysia.

Jaffe, E.S., Harris, N.L., Stein, H., & Vardiman, J.W. (2001). *World Health Organisation classification of tumors: Pathology and genetics of tumours of haematopoietic and lymphoid tissues*. Lyon, France: IARC Press.

Joshi, V.V., & Frei, J.V. (1970). Effects of dose and schedule of methylnitrosourea on incidence of malignant lymphoma in adult female mice. *Journal of National Cancer Institute*, *45*, 335-339.

Kerja, L., & Seidel, H.J. (1986). T-cell markers in the thymus during MNU induced leukemogenesis. *Immunology letters*, *12*, 115-119.

Koestner, A.W., Ruecker, F.A., & Koestner, A. (1977). Morphology and pathogenesis of tumors of the thymus and stomach in Sprague-Dawley rats following intragastric administration of MNU. *International Journal of Cancer*, *20*, 418-426.

Luna, L.G. (1968). *Manual of histologic methods of the Armed Forces Institute of Pathology*. New York: McGraw-Hill.

McCormick, D.L., Rao, K.V.N., Steele, V.E., Lubet, R.A., Kelloff, G.L., & Bosland, M.C. (1999). Chemoprevention of rat prostate carcinogenesis by 9-*cis*-retinoic acid. *Cancer Research*, *59*, 521-524.

Mizoguchi, M., Naito, H., Kurata, Y., Shibata, M.A., Tsuda, H., Wild, C.P., Montesano. R., & Fukushima, S. (1993). Influence of aging on multi-organ carcinogenesis in rats induced by *N*-methyl-*N*-nitrosourea. *Japanese Journal of Cancer Research*, *84*, 139-146.

Morton, D., Bailey, K.L., Stout, C.L., Weaver, R.J., White, K.A., Lorenzen, M.J., & Ball, D.J. (2008). *N*-Methyl-*N*-Nitrosourea (MNU): A positive control chemical for p53+/- mouse carcinogenicity studies. *Toxicologic Pathology*, *36*, 926-931.

Swenberg, J.A., Koestner, A., Wechsler, W., Brunden, M.N., & Abe, H. (1975). Differential oncogenic effects of methylnitrosourea. *Journal of the National Cancer Institute*, *54*, 86-95.

Tuncel, H., Shimamoto, F., Cagatay, P., & Kalkan, M.T. (2002). Variable E-cadherin expression in a MNU-induced colon tumor model in rats which exposed with 50 Hz frequency sinusoidal magnetic field. *Tohoku Journal of Experimental Medicine*; *198*, 245-249.

Uwagawa, S., Tsuda, H., Inoue, T., Tagawa, Y., Aoki, T., Kagawa, M., Ogiso, T., & Ito, N. (1991). Enhancing potencial of 6 different carcinogens on multi-organ tumorigenesis after initial treatment with NMU. *Japanese Journal of Cancer Research*, *82*, 1397-405.